

## Damping of a Unitary Fermi Gas

J. Kinast, A. Turlapov, and J. E. Thomas

*Department of Physics, Duke University, Durham, North Carolina 27708, USA*

(Received 21 February 2005; published 6 May 2005)

We measure the temperature dependence of the radial breathing mode in an optically trapped, unitary Fermi gas of  ${}^6\text{Li}$ , just above the center of a broad Feshbach resonance. The damping rate reveals a clear change in behavior which we interpret as arising from a superfluid transition. We suggest pair breaking as a mechanism for an increase in the damping rate which occurs at temperatures well above the transition. In contrast to the damping, the frequency varies smoothly and remains close to the unitary hydrodynamic value. At low temperature  $T$ , the damping depends on the atom number only through the reduced temperature, and extrapolates to 0 at  $T = 0$ .

DOI: 10.1103/PhysRevLett.94.170404

PACS numbers: 03.75.Ss, 32.80.Pj

Optically trapped, unitary Fermi gases [1,2] test predictions for exotic systems, from nuclear matter [3–5] and quark-gluon plasmas [6] to high temperature superconductors [7]. In a unitary Fermi gas, pair interactions between particles are “strong” in the sense that the zero-energy scattering length is much greater than the interparticle spacing, as achieved by tuning near a Feshbach resonance [1]. Such a gas is believed to exhibit universal features, independent of the microscopic details of the interaction [1,3,8]. At sufficiently low temperatures, unitary Fermi gases comprise normal atoms, noncondensed pairs, and condensed superfluid pairs [9,10]. Fermionic atom pairs are probed in projection experiments [11–13] and in measurements of the pairing gap [14,15]. The anisotropic expansion of a unitary gas [1] and the breathing mode frequencies and damping rates [16–18] provide evidence for superfluid hydrodynamics. Recent measurements of the heat capacity of a unitary gas reveal a transition at a certain temperature [10,19], which has been interpreted as the onset of superfluidity [9,10]. However, in collective mode measurements, a well-defined transition temperature has not been identified, and the scaling of the superfluid damping rate with temperature has not been established. Further, measurements above the transition temperature may determine if the normal phase behaves as a normal Fermi liquid, a normal Fermi gas, or something else.

In this Letter, we report a comprehensive study of the radial breathing mode for a unitary Fermi gas of  ${}^6\text{Li}$ . We measure the frequency and damping rate as a function of an empirical temperature  $\tilde{T}$ . We observe a transition in the behavior of the damping rate at  $\tilde{T} = 0.5$ , corresponding to a reduced temperature of  $T/T_F = 0.35$ . Below  $\tilde{T} = 0.5$ , we observe linear scaling of the damping rate with empirical temperature. The rate extrapolates to zero at zero temperature, as expected for a superfluid. Above  $\tilde{T} = 0.5$ , the behavior deviates strongly from linear scaling. The transition is not accompanied by an abrupt change of the frequency, which remains close to the unitary hydrodynamic value. For  $\tilde{T} \geq 1.0$ , the behavior of the frequency and damping rate is difficult to interpret in terms of binary collisional dynamics or trap anharmonicity. We discuss a

possible explanation in terms of the breaking of noncondensed pairs.

In the experiments, we prepare a degenerate 50-50 mixture of the two lowest spin states of  ${}^6\text{Li}$  atoms by forced evaporation [1] in an ultrastable  $\text{CO}_2$  laser trap [20]. At a bias magnetic field  $B$  of 840 G, just above the center of the Feshbach resonance [21,22], the trap depth is lowered by a factor of  $\approx 580$  in a few seconds [1,16] and then recompressed to 4.6% (for most of the experiments) of the maximum trap depth in 1.0 s and held for 0.5 s to assure equilibrium. To increase the temperature, a controlled amount of energy is added to the gas by releasing the atoms from the trap for a short time and then recapturing the cloud [10,19]. The gas is then allowed to thermalize for 0.1 s.

The radial breathing mode is excited by releasing the cloud and recapturing the atoms after 25  $\mu\text{s}$  (for 4.6% of the maximum trap depth). After the excitation, we let the cloud oscillate for a variable time  $t_{\text{hold}}$ , at the end of which the gas is released and imaged after  $\approx 1$  ms of expansion [16].

Radial breathing mode frequencies  $\omega$  and damping times  $\tau$  are determined from the oscillatory dependence of the released cloud size on  $t_{\text{hold}}$  [16–18]. For each temperature, 60-90 values of  $t_{\text{hold}}$  are chosen in the time range of interest. These values of  $t_{\text{hold}}$  are randomly ordered during data acquisition to reduce systematic error. Three full sequences are obtained and averaged. The averaged data is fit with a damped sinusoid  $x_0 + A \exp(-t/\tau) \sin(\omega t + \varphi)$ . We have obtained oscillation curves at 30 different temperatures, containing data from 6300 repetitions of the experiment.

For most of the data reported, the total number of atoms is  $N = 2.0(0.2) \times 10^5$ . From the measured trap frequencies, corrected for anharmonicity, we obtain for 4.6% of the maximum trap depth:  $\omega_{\perp} = \sqrt{\omega_x \omega_y} = 2\pi \times 1696(10)$  Hz,  $\omega_x/\omega_y = 1.107(0.004)$ , and  $\omega_z = 2\pi \times 71(3)$  Hz, so that  $\bar{\omega} = (\omega_x \omega_y \omega_z)^{1/3} = 2\pi \times 589(5)$  Hz is the mean oscillation frequency and  $\lambda = \omega_z/\omega_{\perp} = 0.045$  is the anisotropy parameter. The typical

Fermi temperature  $T_F = (3N)^{1/3} \hbar \omega / k_B$  of a corresponding noninteracting gas is  $\approx 2.4 \mu\text{K}$ , small compared to the final trap depth of  $U_0/k_B = 35 \mu\text{K}$  (at 4.6% of maximum depth). The coupling parameter of the strongly interacting gas at  $B = 840 \text{ G}$  is  $k_F a \approx -30.0$ , where  $\hbar k_F = \sqrt{2mk_B T_F}$  is the Fermi momentum, and  $a = a(B)$  is the zero-energy scattering length estimated from Ref. [21].

The dimensionless empirical temperature  $\tilde{T}$  is determined by the method implemented in [10,19]: The column density of the cloud is spatially integrated in the axial direction to yield a normalized (integrates to 1), one-dimensional, transverse spatial distribution  $n(x)$ . This distribution is fit to determine the empirical reduced temperature  $\tilde{T}$  using a finite-temperature Thomas-Fermi profile with a fixed Fermi radius, which is measured in a separate experiment at the lowest temperatures [10,19]. The empirical temperature  $\tilde{T}$  is numerically calibrated to the theoretical reduced temperature  $T/T_F$  [9,10]. In Ref. [10], we show that a simple approximation relating  $\tilde{T}$  to  $T/T_F$  is given by

$$\tilde{T} \approx \tilde{T}_{\text{nat}} \equiv \frac{T}{T_F \sqrt{1 + \beta}}. \quad (1)$$

Equation (1) yields accurate values of  $T/T_F$  for  $\tilde{T} \geq 0.45$  and provides a reasonable estimate at lower temperatures, where higher precision can be obtained using the calibration [10,23]. Here  $\beta$  is the unitary gas parameter [1,3,5,24,25], which we recently measured to be  $\beta = -0.49(0.04)$  (statistical error only) [10,19].

The mode frequency provides important information on the state of the system. The frequency versus the empirical temperature for experiments at 4.6% of maximum trap depth is shown in Fig. 1. The figure shows the measured frequencies  $\omega_{\text{meas}}$  (open circles), uncorrected for anharmonicity in the trapping potential, as well as the frequencies after correction (solid dots).

The frequency correction is proportional to the ratio  $\langle \rho^4 \rangle / \langle \rho^2 \rangle$  [26], where  $\rho$  is the transverse radius of the expanded cloud. For a unitary gas under isentropic conditions, we obtain [27]

$$\omega = \omega_{\text{meas}} \left( 1 + \frac{8}{15} \frac{m \omega_x^2}{U_0} \frac{\langle x^4 \rangle}{\langle x^2 \rangle b_x^2} \right). \quad (2)$$

Here, we have assumed that the spatial profile is cigar shaped, with  $(\omega_x - \omega_y)^2 / \omega_\perp^2 \ll 1$ , and that the breathing mode is observed in the  $x$  direction, where  $\langle x^2 \rangle$  is the mean square width of the cloud after the expansion by a scale factor  $b_x$  [1,28]. For 1 ms of hydrodynamic expansion [29], we find  $b_x(1 \text{ ms}) = 13.3$ .

We determine the ratio  $\langle x^4 \rangle / \langle x^2 \rangle$  directly from the measured spatial distributions, by fitting with one-dimensional finite-temperature Thomas-Fermi profiles. The corrected frequencies are displayed in Fig. 1 as solid dots. The frequency error arising from uncertainty in the correction is estimated to be comparable to the statistical error.

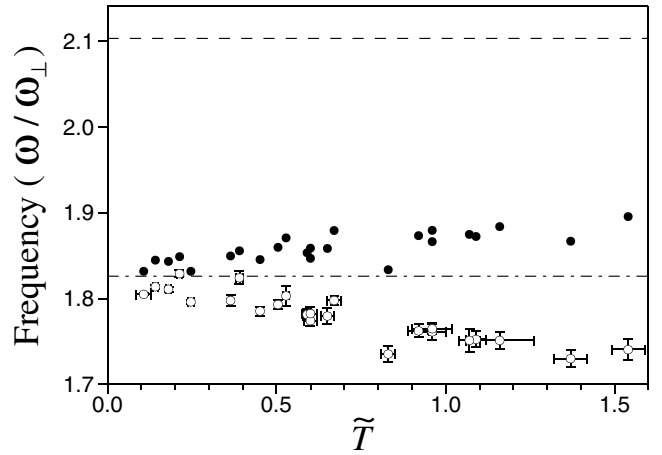


FIG. 1. Frequency  $\omega$  versus empirical reduced temperature  $\tilde{T}$ . Open circles: measured frequencies; Black dots: after correction for anharmonicity using a finite-temperature Thomas-Fermi profile. The dot-dashed line is the unitary hydrodynamic frequency  $\omega_H = \sqrt{10/3} \omega_\perp$ . The dashed line at the top of the scale is the frequency  $2\omega_x$  observed for a noninteracting gas at the lowest temperatures.

The radial breathing frequency varies smoothly over the whole temperature range, and remains close to the value  $\omega_H = \sqrt{10/3} \omega_\perp = 1.83 \omega_\perp$  predicted by hydrodynamic theory for a unitary gas, where  $1/(k_F a) = 0$  [31–37]. Such temperature independence has been observed previously in a Bose-Einstein condensate (BEC) [38]. We find that the corrected frequencies are far from  $2\omega_x = 2.10 \omega_\perp$ , the value observed for a noninteracting gas at the lowest temperatures (dashed line at the top of Fig. 1).

In contrast to the frequency, the damping rate, Fig. 2, reveals a transition in behavior as  $\tilde{T}$  is increased from 0. For  $\tilde{T} \lesssim 0.5$ , the damping rate varies linearly with  $\tilde{T}$  [23]. A linear fit for this temperature range yields

$$\frac{1}{\tau \omega_\perp} = 0.146(0.004) \tilde{T} - 0.0015(0.0014), \quad (3)$$

for the main data set which is taken at 4.6% of maximum trap depth and  $N = 2 \times 10^5$  atoms. The damping rate extrapolates close to zero at zero temperature, similar to that observed in the radial breathing mode of a BEC [38]. The hydrodynamic frequency and decrease in damping with decreasing  $\tilde{T}$  are inconsistent with expectations for a collisionally hydrodynamic gas [for binary collisions,  $1/\tau \propto (T/T_F)^{-2}$ ] [16,30,39,40], and are consistent with a Fermi superfluid [16].

Above  $\tilde{T} = 0.5$ , the damping rate departs strongly from linear scaling with  $\tilde{T}$ . We interpret this behavior as a signature of a phase transition. Using Eq. (1), we find that  $\tilde{T} = 0.5$  corresponds to  $T = 0.35 T_F$ . This is somewhat higher than the temperature  $T = 0.27 T_F$  where a transition is observed in the heat capacity, after temperature calibration [10]. However, it is not clear that the observed change

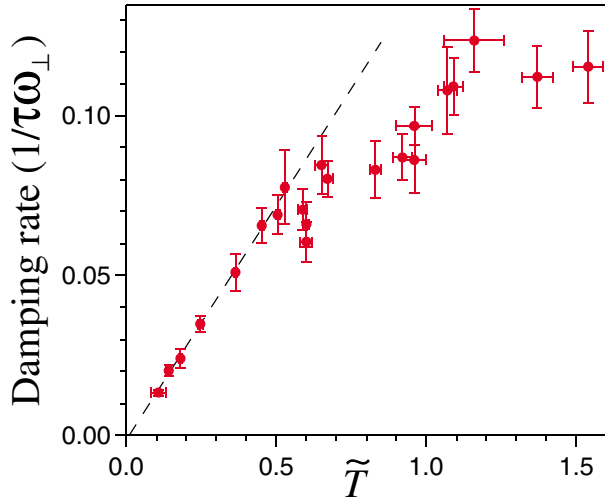


FIG. 2 (color online). Temperature dependence of the damping rate for the radial breathing mode of a trapped  ${}^6\text{Li}$  gas at 840 G, showing a transition in behavior. Solid dots are the main data set taken at 4.6% of maximum trap depth and  $N = 2.0(0.2) \times 10^5$ . The dashed line is Eq. (3) which extrapolates close to zero at zero temperature.

in the behavior of the damping rate should occur at precisely the same temperature as for the change in heat capacity. The two measurements are in reasonable agreement with recent predictions for the superfluid transition temperature,  $T_c = 0.29T_F$  [10] and  $0.31T_F$  [41].

There appears to be a notch in the damping rate near  $\tilde{T} = 0.6$ . The three data points in the notch are taken together with points above and below the notch, and demonstrate reproducible reduction in the damping rate. The three points in the notch fall 2.2–4.1 standard errors below the linear extrapolation at  $\tilde{T} = 0.6$ . By contrast, for the eight points to the left of the notch, the average magnitude of the deviation from linear scaling is 0.3 standard error. This unexpected feature merits further investigation.

For the data points in the range  $0.65 \leq \tilde{T} \leq 1.0$ , i.e., for  $0.45 < T/T_F < 0.71$ , the damping rate appears to be nearly independent of  $\tilde{T}$ . The damping increases for  $1.0 \leq \tilde{T} \leq 1.2$ , i.e., for  $0.71 \leq T/T_F \leq 0.86$ , and then appears to become nearly temperature independent with further increase in  $\tilde{T}$ .

We have examined several scenarios for the behavior of the damping rate for  $\tilde{T} \geq 1.0$ , i.e.,  $T/T_F \geq 0.71$ . The observed damping rates and frequencies appear to be inconsistent with expectations for binary collisions in a normal Fermi gas: Predictions [40] indicate that the damping above  $T/T_F \geq 0.7$  should be varying slowly (on the scale of  $T_F$ ) and decreasing with temperature in this regime. The observed frequency is close to the hydrodynamic value. In contrast, the predicted frequency is close to the noninteracting gas value,  $2\omega_x$ , because the momentum relaxation rate predicted by the binary collision model is too small.

The observed maximum damping rate above  $\tilde{T} = 1.2$  is, however, close to the maximum value for a general relaxation model [30], which occurs in the regime where the gas changes from collisional to collisionless. We find  $1/(\omega_{\perp}\tau)_{\text{max}}$  is  $1/\sqrt{120} \approx 0.09$  for exact cylindrical symmetry, and 0.13 for our trap [29].

If anharmonicity in the trapping potential were causing the increase in damping rate with temperature,  $1/\tau$  would be proportional to the frequency correction, i.e.,  $1/(\omega_{\perp}\tau) \propto m\omega_{\perp}^2\langle x^2\rangle/U_0 \propto k_B T/U_0$ . Then, for our trap conditions, the damping rate would increase rapidly for all  $\tilde{T} \geq 1.0$ , in contrast to observations.

The breaking of noncondensed pairs may contribute to the increase in the damping rate as the temperature is increased. Pair breaking has been suggested [17] as a mechanism for enhanced damping which is observed at magnetic fields above the Feshbach resonance, where the coupling is reduced and the trap-averaged pairing gap  $\langle\Delta\rangle$  decreases below the radial breathing mode excitation energy  $\hbar\omega$  [17,18]. A recent prediction [42] shows that  $\langle\Delta\rangle \approx \hbar\omega$  for  $\tilde{T} \approx 0.1$  ( $T/T_F = 0.12$ ),  $B = 1080$  G ( $1/k_F a = -0.74$ ), and  $\hbar\omega = 0.06k_B T_F$ , the conditions where we have observed enhanced damping [18]. This is consistent with the pair-breaking hypothesis. We find that the region of increasing damping in the current experiments,  $0.71 \leq T/T_F \leq 0.86$ , is close to the temperature range estimated for the vanishing of noncondensed pairs in a unitary gas [9,10,19]. Indeed, a prediction of the trap-averaged gap for a unitary gas [42] shows that  $\langle\Delta\rangle \leq \hbar\omega$  for  $T \geq 0.75T_F$  ( $\tilde{T} \geq 1.06$ ).

We have investigated the possibility that the observed variation of the damping rate with temperature might arise in part from oscillations of different components of the gas at different frequencies. In a Bose-Einstein condensate with a thermal cloud, numerical simulations predict revivals of the net oscillation amplitude, altering the apparent decay rates [43]. In the present experiments, we find no evidence for such revivals, even after increasing the time over which the decay of the mode is observed.

We have examined the dependence of the damping rate on the trap oscillation frequency  $\omega_{\perp}$  and on the number of atoms  $N$ , Fig. 3. Dimensional analysis requires that  $1/\tau = \omega_{\perp} f(T/T_F, N, \lambda)$ , where  $f$  is a dimensionless function.

For fixed  $T/T_F$  (or fixed  $\tilde{T}$ ), we find that the function  $f$  cannot have a strong number dependence for  $\tilde{T} < 0.5$ . For example, it cannot be  $\propto k_B T_F / (\hbar\omega_{\perp}) \propto N^{1/3}$  or its inverse, since the damping rate at 4.6% of maximum trap depth does not change significantly when the number is reduced by a factor of  $\approx 3$ : The damping rate at reduced numbers, open circles in Fig. 3, lies very close to the main data set (dashed line) when plotted versus  $\tilde{T}$ . Hence, it is likely that  $1/\tau$  depends on  $N$  only via the combination  $T/T_F$ , and the most general formula for  $1/\tau$  is then limited to

$$\frac{1}{\tau} = \omega_{\perp} f\left(\frac{T}{T_F}, \lambda\right). \quad (4)$$

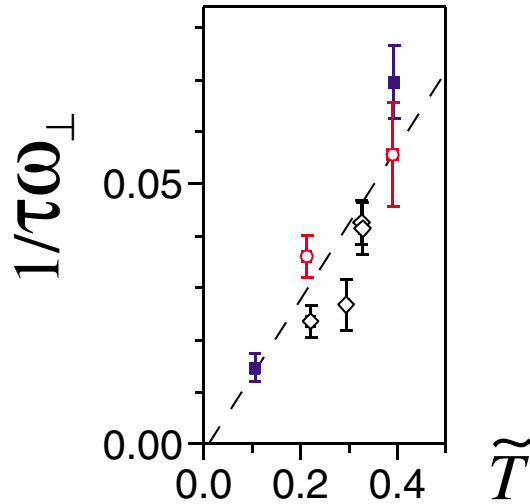


FIG. 3 (color online). Damping rate for the system with scaled parameters: Two solid squares: at 0.85% of maximum trap depth; Four open diamonds: at 19% of maximum trap depth; Two open circles: at 3 times smaller number of atoms and 4.6% of maximum trap depth. The dashed line is Eq. (3) which extrapolates close to zero at zero temperature.

Experimentally, we are not able to test whether the damping rate depends on  $\lambda$ . We have verified that  $1/\tau$  versus  $\tilde{T}$  scales approximately as  $\omega_{\perp}$  by monitoring the breathing mode in the trap at 0.85% of full depth ( $\omega_{\perp} = 728(4)$  Hz, squares in Fig. 3) and at 19% ( $\omega_{\perp} = 3343(20)$  Hz, diamonds). In both cases,  $1/(\omega_{\perp}\tau)$  is close to that of the main data set.

We are indebted to Qijin Chen, Kathy Levin, and Jason Ho for stimulating discussion and for critical reading of the manuscript. We also thank Qijin Chen and Kathy Levin for providing calculations of the pairing gap versus temperature prior to publication. This research is supported by the Physics Divisions of the Army Research Office and the National Science Foundation, the Physics for Exploration program of the National Aeronautics and Space Administration, and the Chemical Sciences, Geosciences and Biosciences Division of the Office of Basic Energy Sciences, Office of Science, U. S. Department of Energy.

\*jet@phy.duke.edu

- [1] K. M. O'Hara *et al.*, Science **298**, 2179 (2002).
- [2] J. E. Thomas and M. E. Gehm, Am. Sci. **92**, 238 (2004).
- [3] H. Heiselberg, Phys. Rev. A **63**, 043606 (2001).
- [4] G. A. Baker, Jr., Phys. Rev. C **60**, 054311 (1999).
- [5] J. Carlson *et al.*, Phys. Rev. Lett. **91**, 050401 (2003).
- [6] P. F. Kolb and U. Heinz, *Quark Gluon Plasma 3* (World Scientific, Singapore, 2003), p. 634; see nucl-th/0305084; E. Shuryak, Prog. Part. Nucl. Phys. **53**, 273 (2004).
- [7] Q. Chen *et al.*, cond-mat/0404274.
- [8] T.-L. Ho, Phys. Rev. Lett. **92**, 090402 (2004).
- [9] Q. Chen, J. Stajic, and K. Levin, cond-mat/0411090.

- [10] J. Kinast *et al.*, Science **307**, 1296 (2005).
- [11] C. A. Regal, M. Greiner, and D. S. Jin, Phys. Rev. Lett. **92**, 040403 (2004).
- [12] M. W. Zwierlein *et al.*, Phys. Rev. Lett. **92**, 120403 (2004).
- [13] M. W. Zwierlein *et al.*, cond-mat/0412675 [Phys. Rev. Lett. (to be published)].
- [14] C. Chin *et al.*, Science **305**, 1128 (2004).
- [15] M. Greiner, C. A. Regal, and D. S. Jin, Phys. Rev. Lett. **94**, 070403 (2005).
- [16] J. Kinast *et al.*, Phys. Rev. Lett. **92**, 150402 (2004).
- [17] M. Bartenstein *et al.*, Phys. Rev. Lett. **92**, 203201 (2004).
- [18] J. Kinast, A. Turlapov, and J. E. Thomas, Phys. Rev. A **70**, 051401(R) (2004).
- [19] J. Kinast, A. Turlapov, and J. E. Thomas, cond-mat/0409283.
- [20] K. M. O'Hara *et al.*, Phys. Rev. Lett. **82**, 4204 (1999).
- [21] M. Bartenstein *et al.*, Phys. Rev. Lett. **94**, 103201 (2005).
- [22] C. H. Schunck *et al.*, Phys. Rev. A **71**, 045601 (2005).
- [23] For  $\tilde{T} \leq 0.45$ , we find  $\sqrt{1 + \beta\tilde{T}} = 1.8(T/T_F)^{3/2}$ ; see Ref. [10].
- [24] M. E. Gehm *et al.*, Phys. Rev. A **68**, 011401(R) (2003).
- [25] A. Perali, P. Pieri, and G. C. Strinati, Phys. Rev. Lett. **93**, 100404 (2004).
- [26] This frequency shift was first derived by S. Stringari (private communication).
- [27] We ignore here an additional small correction  $\lambda^2 \langle z^2 \rho^2 \rangle / (4 \langle \rho^2 \rangle)$ , which would increase the coefficient in Eq. (2) from  $8/15$  to  $8/15 + 1/12$ . However, at the highest temperatures, the next order correction is also  $\approx 10\%$  of the first order and of the opposite sign.
- [28] C. Menotti, P. Pedri, and S. Stringari, Phys. Rev. Lett. **89**, 250402 (2002).
- [29] We have generated a complete locus plot of the breathing mode frequency  $\omega$  and damping rate  $1/\tau$  for our trap, where  $\omega_x \neq \omega_y$ , using a general relaxation model [30]. Independent of the mechanism for momentum relaxation, we find that momentum space damping rates compatible with our measured frequencies yield  $b_x$  within 2% of the hydrodynamic value, even for our largest  $1/\tau$ .
- [30] D. Guéry-Odelin *et al.*, Phys. Rev. A **60**, 4851 (1999).
- [31] S. Stringari, Europhys. Lett. **65**, 749 (2004).
- [32] H. Heiselberg, Phys. Rev. Lett. **93**, 040402 (2004).
- [33] H. Hu *et al.*, Phys. Rev. Lett. **93**, 190403 (2004).
- [34] Y. E. Kim and A. L. Zubarev, Phys. Lett. A **327**, 397 (2004).
- [35] Y. E. Kim and A. L. Zubarev, Phys. Rev. A **70**, 033612 (2004).
- [36] N. Manini and L. Salasnich, Phys. Rev. A **71**, 033625 (2005).
- [37] A. Bulgac and G. F. Bertsch, Phys. Rev. Lett. **94**, 070401 (2005).
- [38] F. Chevy *et al.*, Phys. Rev. Lett. **88**, 250402 (2002).
- [39] L. Vichi, J. Low Temp. Phys. **121**, 177 (2000).
- [40] P. Massignan, G. M. Bruun, and H. Smith, Phys. Rev. A **71**, 033607 (2005).
- [41] A. Perali *et al.*, Phys. Rev. Lett. **92**, 220404 (2004).
- [42] The pairing gap has been calculated as a function of  $T/T_F$  and  $1/(k_F a)$ , Q. Chen and K. Levin (private communication).
- [43] B. Jackson and C. S. Adams, Phys. Rev. A **63**, 053606 (2001).